

Supporting Information

Single-molecule study on conformational dynamics of M.HhaI

Shanshan He,^{a,b} Chen Yang,^{a,b} Sijia Peng,^c Chunlai Chen^c and Xin Sheng Zhao^{*a,b}

a. Beijing National Laboratory for Molecular Sciences, State Key Laboratory for Structural Chemistry of Unstable and Stable Species, and Department of Chemical Biology, College of Chemistry and Molecular Engineering, Peking University, Beijing 100871, China.

b. Biomedical Pioneering Innovation Center (BIOPIC), Peking University, Beijing 100871, China.

c. School of Life Sciences, Tsinghua-Peking Joint Center for Life Sciences, Beijing Advanced Innovation Center for Structural Biology, Tsinghua University, Beijing 100084, China.

E-mail: zhaoxs@pku.edu.cn

Contents:

1. Materials and Methods.....	1
2. Supplementary Table	5
3. Supplementary Figures	5
4. References	10

1. Materials and Methods

Materials

AdoMet and AdoHcy were purchased from Sigma-Aldrich. DNA substrates were ordered and synthesized from Invitrogen and Takara, the single-stranded oligonucleotides used in this work are listed in Table S1.

Expression, purification, and mutagenesis of M.HhaI

The pET32a vector carrying the His6-tagged M.HhaI was transformed into and expressed in NEB T7 Express *I^q* *Escherichia coli* cells. Cells were grown in 1 L of Lysogeny broth (LB) medium containing 100 mg mL⁻¹ ampicillin at 37 °C. Protein expression was induced with 0.5 mM IPTG at OD₆₀₀=0.6. Induction proceeded at 15 °C for 15 h before the cells were harvested by centrifugation. Cells pellets were lysed by ultrasonication in 40 mL of buffer A (40 mM sodium phosphate, 400 mM NaCl, 10 mM imidazole, pH 7.0). The lysate was clarified by centrifugation and the supernatant was loaded on a HisTrapTM HP column (GE Healthcare) pre-equilibrated in buffer A. After the lysate had been loaded, nonrelated proteins were washed out with buffer B (40 mM sodium phosphate, 800 mM NaCl, 40 mM imidazole, pH 7.0). Then the M.HhaI protein was eluted with buffer C (40 mM sodium phosphate, 200 mM NaCl, 250 mM imidazole, pH 7.0). Then the eluted fraction was concentrated using 10 kD Centriprep (Millipore) and desalted by three tandem HiTrapTM desalting columns (GE Healthcare) into buffer D (50 mM Tris-HCl and 50 mM NaCl, pH 8.0). The outflow containing protein

was directly loaded on a HiTrap™ Q FF column (GE Healthcare) pre-equilibrated with buffer D. The salt concentration of flow was gradually increased by adjusting the ratio of buffer D and buffer E (50 mM Tris-HCl and 1000 mM NaCl, pH 8.0). The target protein was collected when buffer E took 10% of flow. The collected fraction was concentrated and desalted into the T50 buffer (50 mM Tris-HCl, 50 mM NaCl, 1 mM EDTA, pH 7.5), and was then frozen and stored at -80 °C.

Fluorescent dyes labelling on M.HhaI

Labelling of the site-directed cysteine mutants of M.HhaI with C81S mutation by FRET pair dyes, AF555 and AF647, was done by first reducing cysteine residues with 10-fold molar excess of tris-2-carboxyethyl-phosphine (TCEP) in 50 mM sodium phosphate (pH 7.0), 100 mM NaCl at 15 °C for 30 min. 1.5-fold molar excess of AF555-maleimide (Life Technology) and 2-fold molar excess of AF647-maleimide (Life Technology) were mixed and then added to ~100 μM M.HhaI protein solution. Then the solution was oscillated at 300 rpm in the dark at 15 °C for 5 h. Excess dyes were removed by passing over four tandem HiTrap™ desalting columns pre-equilibrated with buffer F (100 mM sodium phosphate, 100 mM NaCl, pH 7.5). The absorbance of the protein solution at 280 nm (for proteins), 556 nm (for AF555) and 655 nm (for AF647) was detected to determine protein concentration and the labelling efficiency for each dyes. The extent of labelling was greater than 80% for each dye in most samples. When LD550-MAL (Lumidyne Technologies) and LD650-MAL (Lumidyne Technologies) were used, the labelling reaction followed the same process.

Fluorescent labelling of M.HhaI variants containing Cys81 was achieved through blocking the active Cys81 site with DNA during labelling reaction. 10 μM M.HhaI was mixed with 20 μM Aba-DNA_{hp} first. Then 1.5-fold molar excess of AF555-maleimide and 2-fold molar excess of AF647-maleimide were added to the solution. After that, the solution was oscillated at 300 rpm in the dark at 37 °C for 0.5 h. Finally, the free dyes and DNA were removed by diluting the product solution into T1000 buffer and concentrated with Centriprep for multiple cycles.

Circular dichroism (CD) spectroscopy experiments

The CD spectra were measured for the wild-type M.HhaI, three mutants (142-210, 51-142, 90-210) and their dye labelled products. Experiments were conducted on a Jasco J-815 spectrometer using a 10 mm path length quartz cuvette. Far-UV CD spectra (200–260 nm) for each sample were recorded at 24 °C. M.HhaI was diluted into T50 buffer, with the final concentration being 5 μM. T50 buffer was detected as background and was subtracted during the sample measurement. The CD spectra of wild type M.HhaI in T1000 buffer, and in T50 buffer with 8 M urea were also measured to examine its structure in the folded and denatured states.

Reaction with F-DNA

10 μM M.HhaI with Cys81 reserved was mixed with 20 μM F-DNA and 200 μM AdoMet in T50 buffer. Then, the solution was incubated at 37 °C for 2 h. After that, fluorescent dyes were added to the solution. The dyes labelling reaction proceeded at 37 °C for 0.5 h. After that, all the free small molecules were removed as above.

Biotinylation and immobilization of M.HhaI

For immobilization, an AviTag (GLNDIFEAQKIEWHE) was introduced to the carboxyl terminal of M.HhaI. Biotinylation reaction was performed under the instructions of commercial BirA enzyme

(GeneCopoeia). 40 μM M.HhaI was added to reaction solution with 50 μM D-biotin, 10 mM MgOAc, 50 mM Bicine (pH 8.3) and 45 U/ μL BirA. The catalytic reaction proceeded at 30 $^{\circ}\text{C}$ for 1 h.

Free biotin was removed in the same way as free dyes separation described above. The biotinylation efficiency was quantified by normal SDS-PAGE. 10 μL biotinylated protein sample was added with excess streptavidin (YEASEN Shanghai), and another sample was added with the same volume of H_2O as control. 10 μL of each samples were loaded on two lanes of SDS-PAGE. The temperature was kept low during the run to retain the complex of streptavidin and biotin conjugates. The gel was stained with coomassie blue and visualized. Degree of biotinylation was determined by quantifying intensity of free M.HhaI band in two lanes. With the addition of streptavidin, intensity of free protein band decreased due to forming a bigger complex.

The procedure of immobilization of M.HhaI is similar to that of DNA as described before.¹ The coverslip (Fisher Scientific, Cover Glass 22×22 mm²) used for immobilization was cleaned by acetone, 1 M KOH, and piranha solution successively. Then, it was silanized and PEG functionalized. The ratio of Bio-PEG-5000 to mPEG-5000 (Laysan Bio) was 1:40. A hybridization chamber (Life Technologies, Secure-Seal) or another coverslip was put on the surface to form sample cell. By sequentially flowing 0.1 mg/mL streptavidin, wash buffer, 200 pM biotinylated M.HhaI, and wash buffer again through the cell, mono-dispersed M.HhaI molecules were immobilized on the coverslip surface through biotin-streptavidin interaction.

Single-molecule FRET experiments in aqueous solution

Fluorescently labelled M.HhaI was diluted into desired solution, with the final concentration being about 40 pM. 0.02% (v/v) Tween-20 (Surfact-Amps 20, Life Technology) was added to solution to diminish glass surface absorption. 40 μL sample solution was added to sample cell built by a hybridization chamber and a coverslip, and then got sealed.

The experiments were conducted on a home-built inversed confocal fluorescence microscope as described before.² 100 μW 532 nm laser was used to excite fluorescent probes in sample solution through an oil-immersion objective (Nikon, 100 \times , NA=1.4). The emitted fluorescence was divided to donor and acceptor channels by a dichroic mirror, then filtered by according spectral filters, and finally be detected by two photon counting avalanche photodiodes (APD) separately. The bin time for data collection was 1 ms, and the time length for each collection was 30 min.

Only effective signals were selected by setting a threshold of 50 photons ms^{-1} for the acceptor and donor channels together. The apparent FRET efficiency (E_{app}) were calculated as the ratio of the detected photon numbers in the acceptor channel over that in the acceptor and donor channels together. The E_{app} distribution histogram was obtained and normalized according to the total events.

FRET efficiency correction

In aqueous smFRET experiments above, the true FRET efficiency (termed as E) for all the mutants in the DNA bound state were calculated via equation,

$$E = \frac{(n_A - n'_A) - \beta(n_D - n'_D)}{(n_A - n'_A) + \gamma(n_D - n'_D)}$$

where n_D and n_A are detected photon numbers in the donor and acceptor channel. n'_D and n'_A are the background noises of donor and acceptor channels which were obtained by Poisson fitting of the

histogram of photon counts in every millisecond. β is the cross-talk of the donor emission into the acceptor channel and was measured by detecting the leakage of AF555. γ accounts for the differences in quantum yield and detection efficiency between the donor and the acceptor. γ is usually calculated as the ratio of change in the acceptor intensity (Δn_A) to change in the donor intensity (Δn_D) upon acceptor photobleaching, which can be determined by performing single-molecule detection on immobilized molecules, or from reference molecules of known E .

Single-molecule FRET experiments on an objective-based total internal reflection fluorescence (TIRF) microscope

For the study of global conformational dynamics, experiments were conducted on an objective-type TIRF microscope as described before.³ M.HhaI molecules were immobilized on glass surface. Here, LD550 and LD650 were used instead of AF555 and AF647 to get stable photon trace with longer observation time. Measurements were conducted for M.HhaI under different NaCl concentrations, varying from 0 mM to 1000 mM while the rest compositions of buffer kept as 50 mM Tris-HCl and 1 mM EDTA, pH 7.5 (denoted as T0 to T1000). An oxygen scavenging system, containing 3 mg/mL glucose, 100 μ g/mL glucose oxidase (Sigma-Aldrich), 40 μ g/mL catalase (Roche), and 1.5 mM 6-hydroxy-2,5,7,8-tetramethyl-chromane-2-carboxylic acid (Trolox, Sigma-Aldrich), was added to the detection buffer right before measurement. 30 mW 532 nm laser was used to excite molecules on surface. The emitted fluorescence of donor and acceptor was collected separately by an EMCCD camera, with collection rate of 40 frames s⁻¹. Fluorescence traces for each molecules were extracted as described before.³

The bleached traces were removed first. The equilibrium constant K of the transition reaction was calculated as ratio of the areas obtained by Gaussian fitting of the histogram of E_{app} . Transition from unfold state to prefold state was designated as the forward reaction. FRET-FCS technique was used to get the relaxation time (τ_R) of the transition reaction by applying single exponential fitting on the cross correlation curve (G_{AD}) of donor and acceptor photon traces. The second order cross correlation curve G_{AD} was calculated via equation,

$$G_{AD}(t) = \frac{\langle n_A(0)n_D(t) \rangle}{\langle n_A \rangle \langle n_D \rangle}$$

where $n_A(0)$ is photon number in the acceptor channel at time zero and $n_D(t)$ is photon number in the donor channel at time t . $\langle n_A \rangle$ and $\langle n_D \rangle$ are mean of n_A and n_D respectively. Then, the curve G_{AD} was fitted with equation,

$$G_{AD}(t) = 1 + \alpha_{AD} e^{-t/\tau_R}$$

where τ_R is the relaxation time of reaction, which is equal to $1/(k_+ + k_-)$. The cross correlation curves of 142-210 mutant in T0 to T1000 buffer, with corresponding fitting curves, were shown in Fig. S12.

Single-molecule FRET experiments on scanning confocal fluorescence microscope

For the study of loop conformational dynamics, experiments were conducted on a home-built scanning confocal fluorescence microscope as described before.⁴ Briefly, a piezo stage were equipped

on a conventional confocal microscope. Fluorescent probes on mono-dispersed M.HhaI were excited by 5 μ W 532 nm laser beam. The emitted fluorescence of donor and acceptor was separated spectrally by a dichroic mirror, and then got filtered and detected separately by two APDs. After immobilization of M.HhaI, desired detection buffer with oxygen scavenging system was added to the sample cell. The sample cell was sealed and put on to the microscope to get measurements. Firstly, we determined the localizations of immobilized M.HhaI molecules by scanning a $20 \times 20 \mu\text{m}^2$ surface area with a scanning speed of 2 $\mu\text{m/s}$ to get the fluorescence image (100×100 pixels). Then, the central position of each molecule in the image was identified. After that, the laser focus was moved on top of the molecules sequentially to collect the fluorescent traces for both the donor and acceptor channels. A 12 s fluorescent trace with a time resolution of 20 μs was collected for each molecule by using a correlator (Correlator.com, Flex 02-01D). Four areas were scanned, with average 50 effective fluorescence traces recorded in each area. Signals from bleached dyes were thrown away first, and the rest parts were pierced together as one trace.

We use the combination of second and third order FRET-FCS technique to determine the equilibrium constant K .¹ The second order cross correlation curve G_{AD} was calculated and fitted via equations mentioned above, and the third order cross correlation curves were calculated via equations,

$$G_{AAD}(t) = \frac{\langle n_A(0)n_A(t_1)n_D(t) \rangle}{\langle n_A \rangle \langle n_A \rangle \langle n_D \rangle} \quad \text{and} \quad G_{DDA}(t) = \frac{\langle n_D(0)n_D(t_1)n_A(t) \rangle}{\langle n_D \rangle \langle n_D \rangle \langle n_A \rangle}$$

where $t_1 = 20 \mu\text{s}$. Then the correlation curves were fitted with equations,

$$G_{AAD}(t) = A_{AAD} \times \left(1 + \alpha_{AAD} e^{-t/\tau_R}\right) \quad \text{and} \quad G_{DDA}(t) = A_{DDA} \times \left(1 + \alpha_{DDA} e^{-t/\tau_R}\right)$$

The equilibrium constant K and E_{app} corresponding to open and closed states, $E_{\text{app}}^{\text{open}}$ and $E_{\text{app}}^{\text{closed}}$, were determined by using α_{AD} , α_{AAD} and α_{DDA} . Details of the calculation process were described in our previous work.¹

2. Supplementary Table

Table S1 The single-stranded oligonucleotides used in this work

Name of dsDNA		Sequence	Source
SP_DNA	For	5'-ATGTTGTGGGTAAGCGCATAATACTAAAGC-3'	Invitrogen
	Rev	5'-GCTTTAGTATTATGCGCTTACCCACAACAT-3'	
NS_DNA	For	5'-ATGTTGTGGGTAATATATAATACTAAAGC-3'	Invitrogen
	Rev	5'-GCTTTAGTATTATATATTTACCCACAACAT-3'	
F-DNA	For	5'-ATGTTGTGGGTAAG/5-F-dC/GCATAATACTAAAGC-3'	Takara
	Rev	5'-GCTTTAGTATTATG/5-Me-dC/GCTTACCCACAACAT-3'	
Aba-DNA_hp	Hairpin	5'-CATGG/idSp/GCAGTGTTCCTACTGCGCCATG-3'	Invitrogen

3. Supplementary Figures

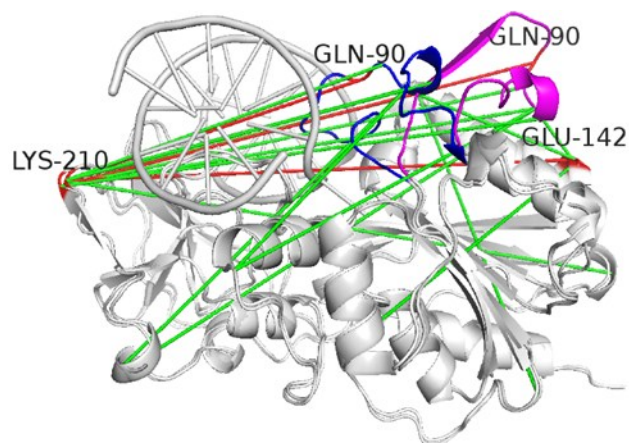


Figure S1. Overlap of crystal structures of apo M.HhaI (1HMY) and DNA bound M.HhaI (5MHT). The catalytic loop is open in apo M.HhaI (magenta) and closed in DNA bound M.HhaI (blue). The locations of 13 FRET pairs were linked by lines. The lines for the extensively used 90-210 and 142-210 mutants are in red and others in green.

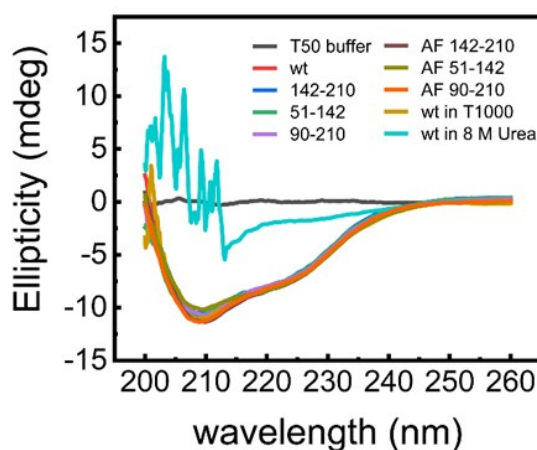


Figure S2. CD spectra of different mutants of M.HhaI and M.HhaI in different conditions. T50 buffer refers to the baseline by sampling T50 buffer as background. M.HhaI was measured in T50 buffer if not noted. wt refers to wild-type M.HhaI. wt in T1000 and wt in 8 M urea were measured in T1000 buffer and T50 buffer with 8 M urea, with according buffer as background. 142-210, 51-142 and 90-210 are mutants without dye labelling. AF 142-210, AF 51-142 and AF 90-210 are respective mutants doubly labelled with dyes AF555 and AF647. The CD spectra of all the mutants show no significant difference from that of wt M.HhaI in T50 buffer, suggesting that mutation and dye labelling do not disturb the structure of M.HhaI. The comparison shows that, except for M.HhaI in 8 M urea which is fully denatured, all other samples in different conditions maintain their secondary α helix and β sheet structures.

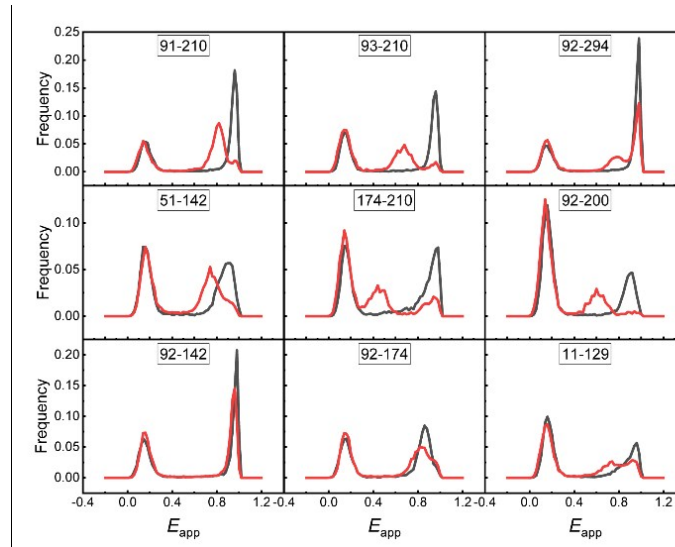


Figure S3. FRET histograms of all other 9 mutants in apo M.HhaI (gray) and in DNA bound M.HhaI (red). Without DNA, all the mutants exhibited similar high FRET peaks. After binding with DNA, lower FRET peaks appeared with the peak position dependent on the distance of the labelled residue pair.

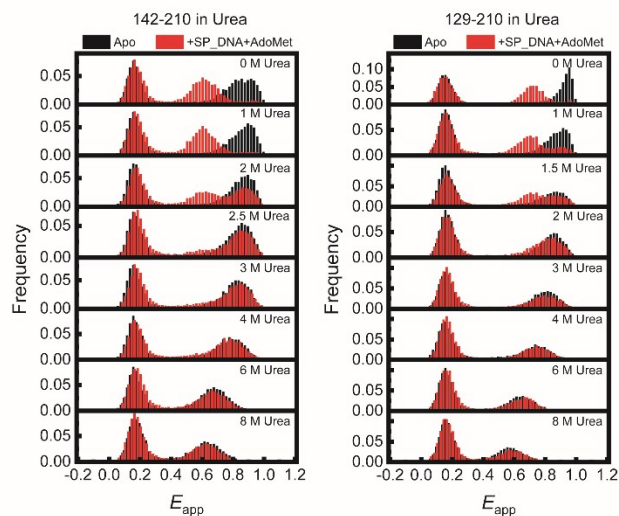


Figure S4. FRET histograms of 142-210 (left) and 129-210 (right) mutants in T50 buffer with different concentrations of urea. With the increase of urea concentration, M.HhaI bound with DNA showed two E_{app} peaks in the process, with the lower one representing the ordered M.HhaI and the higher one representing the disordered M.HhaI, and the transfer between the lower E_{app} peak and higher E_{app} peak representing the phase transition between the two states. In the same conditions, apo M.HhaI only showed one peak shifting towards lower E_{app} due to the conformational expansion caused by urea, which is the typical denaturation pattern of the disordered proteins.²

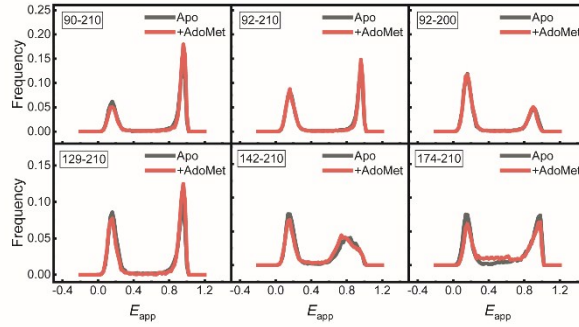


Figure S5. FRET histograms of apo M.HhaI (gray) and M.HhaI with 200 μ M AdoMet (red). The presence of AdoMet does not change the overall structure of DNA free M.HhaI.

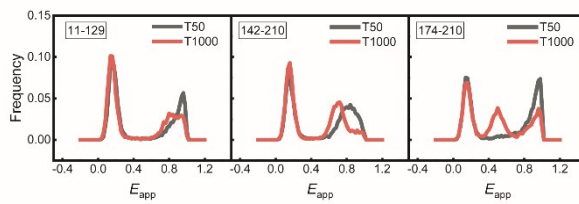


Figure S6. FRET histograms of three M.HhaI mutants, 11-129, 142-210 and 174-210, in apo M.HhaI in T50 (gray) and T1000 buffers (red). Lower E_{app} peak appears in T1000 buffer.

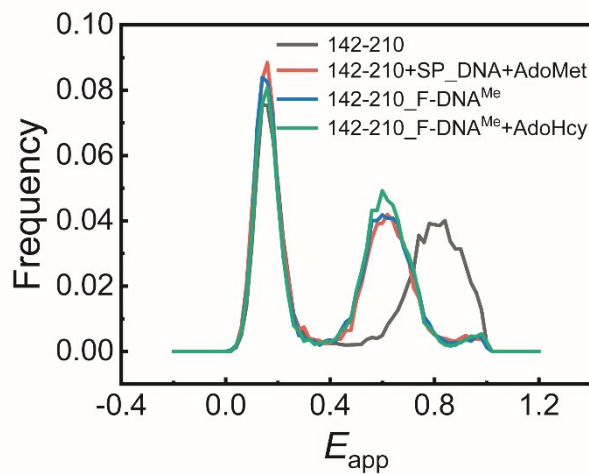


Figure S7. FRET histograms of 142-210 mutant at different conditions in T50 buffer. Apo 142-210 (gray), 142-210 bound with SP_DNA and AdoMet (red), 142-210_F-DNA^{Me} (blue) and 142-210_F-DNA^{Me} with AdoHcy (green). The covalent bond does not influence the folded conformation of M.HhaI in T50 buffer.

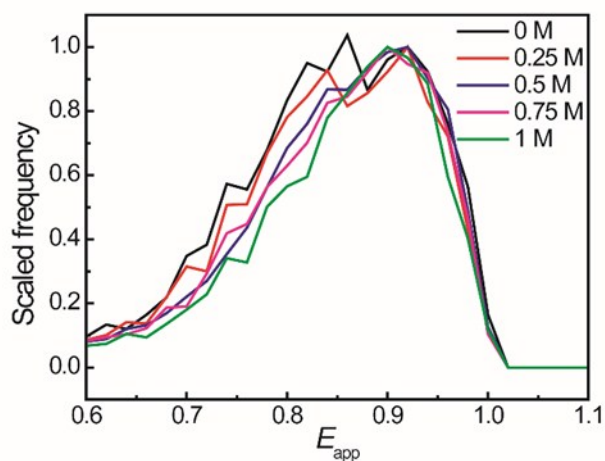


Figure S8. FRET histograms of apo 142-210 in T50 buffer from 0 M to 1 M urea. A state less stable than the folded state diminishes quickly as the increase of urea concentration.

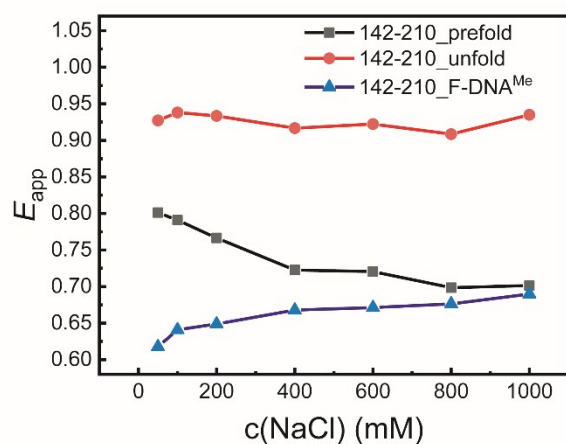


Figure S9. The peaks of E_{app} of the prefold and unfold states in apo 142-210 and that of folded state in 142-210_F-DNA^{Me} in T50 to T1000 buffers. With the increase of salt concentration, The E_{app} of the prefold state of apo 142-210 decreases and meets with that of folded state of 142-210_F-DNA^{Me}. The E_{app} of the unfold state of apo 142-210 hardly change with the increase of salt concentration.

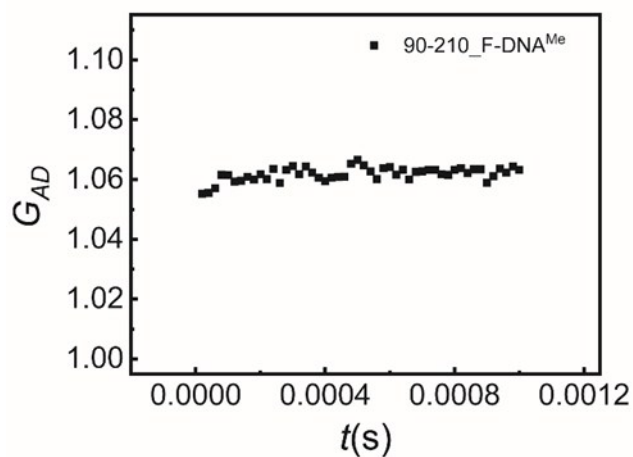


Figure S10. The second order correlation curve G_{AD} between donor and acceptor of covalently bound 90-210_F-DNA^{Me} complex in T50 buffer. No clear anti-correlation can be observed.

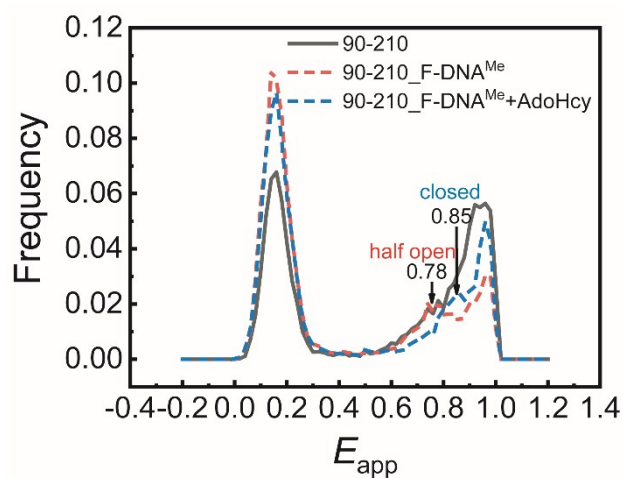


Figure S11. FRET histograms of apo 90-210 (gray solid line), binary complex of 90-210_F-DNA^{Me} (red dashed line) and ternary complex of 90-210_F-DNA^{Me}·AdoHcy (blue dashed line) in T1000 buffer.

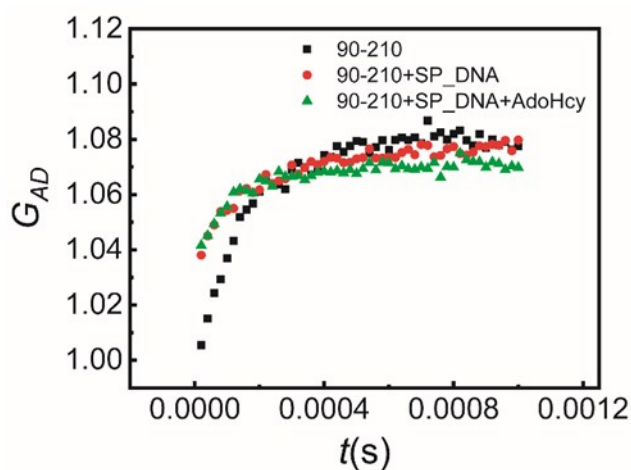


Figure S12. The second order cross correlation curves G_{AD} of the binary complex of M.HhaI·SP_DNA (red) and the ternary complex of M.HhaI·SP_DNA·AdoHcy (green) in T50 buffer. To compare, the cross correlation curve G_{AD} of apo 90-210 in T1000 buffer is also shown (black).

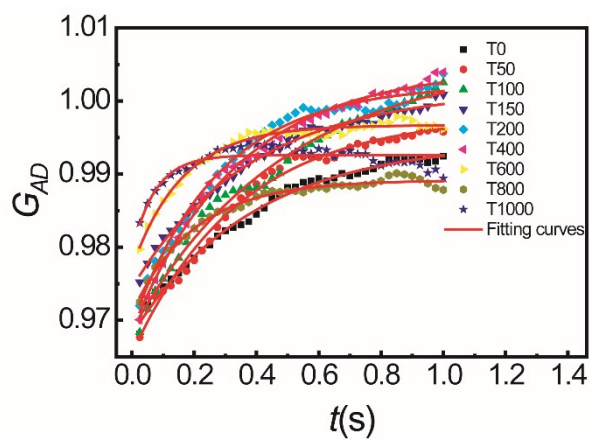


Figure S13. The second order cross correlation curves G_{AD} of 142-210 in T0 to T1000 buffer. Fitting curves were shown as red lines.

4. References

- 1 L. Meng, S. He and X. S. Zhao, *J. Phys. Chem. B*, 2017, **121**, 11262-11272.
- 2 G. Li, C. He, P. Bu, H. Bi, S. Pan, R. Sun and X. S. Zhao, *ACS Chem. Biol.*, 2018, **13**, 1082-1089.
- 3 S. Peng, R. Sun, W. Wang and C. Chen, *Angew. Chem. Int. Ed.*, 2017, **56**, 6882-6885.
- 4 H. Bi, Y. Yin, B. Pan, G. Li and X. S. Zhao, *J. Phys. Chem. Lett.*, 2016, **7**, 1865-1871.